

# A Compact, Fiber-Pigtailed, Terahertz Time Domain Spectroscopy System

**D. Zimdars, J. V. Rudd, and M. Warmuth**

Picometrix, Inc., P. O. Box 130243, Ann Arbor, MI 48113-0243

## 1. INTRODUCTION

Terahertz time-domain spectroscopy (TDS) is a field that has been steadily growing in research labs over the last 11 years<sup>1</sup> with demonstrated spectroscopic applications in semiconductors,<sup>2</sup> liquids,<sup>3,4</sup> and gases,<sup>5</sup> as well as more recent applications based on 2D-imaging.<sup>6</sup> However, even with the interest outside of the ultrafast community given to terahertz spectroscopy and imaging (such as the system initially developed by Nuss and co-workers and popularized as “T-Rays” ),<sup>7</sup> the commercialization of a THz TDS system has been hindered by its complexity. In order to build a TDS system, skills in ultrafast lasers and optics, semiconductor physics, and sub-millimeter waves optics are required. Even if all of the individual components, from the photoconductive antennas to the silicon lenses, were available for purchase, the resulting system would not be useful in most manufacturing or even laboratory environments due to the complexity and instability of free-space optical systems. For these technical reasons, it has been simply not feasible, until now, to take advantage of THz spectroscopy techniques outside of specialized laser science laboratories.

In order to make T-Rays available for general use in the labs of all scientists, we have designed and built a fiber-delivered T-Ray system. The central enabling technology of the Picometrix system revolves around two fiber-pigtailed, hermetically sealed modules that work as the T-Ray transmitter and receiver. These devices are installed inside two larger cases that hold not only the electronics necessary for the modules, but also the millimeter wave optics used to collect and collimate the T-Ray beams. Two fiber-optic and electrical umbilical cords attach these cases to a control box, which contains the computer-controlled, fiber-delivered delay system as well as the fiber optic splitter and optical monitors. Finally, an advanced computer program gives the user the ability to control the entire system and take data without having to align any optics beyond the input fiber. This system represents a major leap forward in the accessibility of ultrafast optics to the general research community as well as a first step in getting this extremely useful tool into more general use.

## 2. THE T-RAY SYSTEM

Figure 1 shows a working fiber-pigtailed terahertz system, while Figure 2 shows a schematic of the system, detailing the components inside each of the boxes. While the group velocity dispersion control (GDC), in the upper right corner of the picture, and the

laser (not shown in Figure 1), must be coupled by free-space optics the remainder of the system is free of the need for an optical table. The control box in particular can sit on a shelf or the floor and not take up valuable space on an optical table. The terahertz cases must be aligned in order to maximize both their signal and their bandwidth, but the required accuracy can be obtained and kept with a simple optical rail and inexpensive alignment components as shown in Figure 1. Furthermore, once the desired alignment for one's particular measurement is determined a mounting bracket can be machined for these two cases, which will then lock them in place for future use.

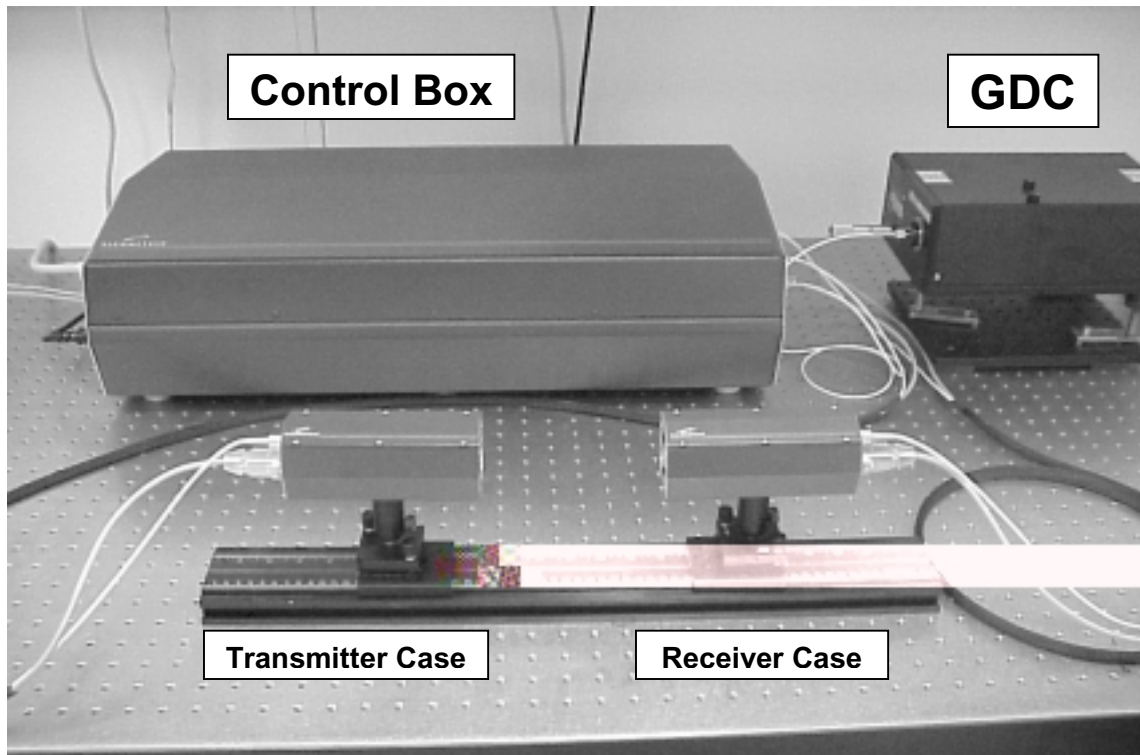


**Figure 1.** The major components of the TDS T-Ray spectroscopy system, less the femtosecond laser and control computer. With the exception of the GDC in the upper right, the other three components do not necessarily have to be on an optical table. The components necessary for imaging are also not shown.

The photoconductive system is powered by a 100-fs laser that works between 750-850 nm and delivers at least 20 mW of optical power. This laser then double-passes a grating-dispersion compensator (the GDC) that imparts negative group-velocity dispersion (GVD) onto the pulse, stretching it to a length of about 5 ps. This stretched pulse is then coupled into a 780-nm singlemode fiber, which delivers the pulse to the control box. The positive GVD of the 5-meters of fiber in our system adds to this negative GVD, compressing the pulse as it travels along the fiber to the terahertz transmitter (Tx) and receiver (Rx). Although the third-order dispersion is additive in these two systems, this only becomes a problem for pulse widths below about 70 fs

and/or fiber lengths greater than about 10 meters. By using a rugged laser that has low variability over time, high-efficiency gratings, as well as by controlling the beam dimensions, GDC systems with 80% of the laser power being coupled into the singlemode fiber have been demonstrated.<sup>8</sup> Since our output electrical signal saturates when optical powers greater than about 10 mW are coupled into the input fiber, this corresponds to only 12.5 mW of total power needed to run the system.

Once the light is in the optical fiber it is taken to the control box, where it is then split into two beams. The first (the pump) is sent directly to the T-Ray transmitter, while the second (the probe) is delivered via fiber to the dual delay system. The delay rail consists of an approximately 20 Hz scanner that has an excursion of 40 ps sitting on top of a stepper-motor rail with a total travel corresponding to 1 ns and speeds ranging from 5-50 ps/sec. This probe pulse is then coupled back into a fiber and delivered to the T-Ray receiver. Both output fibers go through a 99/1 splitter, which picks off 1% so that the user can monitor the power delivered to the transmitter and the receiver by looking at the calibrated readouts in the software.

The two-meter long optical cables deliver the short pulses to the cases while the electrical cables deliver bias voltages to both the receiver amplifier and the transmitter as well as transmit the received signal back to the control box for processing by the computer. Both cases hold their respective fiber-pigtailed module in alignment with the collimating lens such that the terahertz beam exiting the cases has no spatial chirp and is parallel to the case itself. The lenses are 1.5" in diameter with a 3" focal length, and may be made from high-resistivity silicon so that the T-Ray radiation is not absorbed or dispersed by the lens material, or from high density polyethylene for low Fresnel loss. The receiver case also contains a circuit board with the signal amplifier. Finally, the beam path inside the cases is purged with dry nitrogen and sealed in order to eliminate water vapor absorption in this part of the beam.

The T-Ray beam path between the two cases can be used collimated to go through, or reflect off of, large samples, or the user can introduce two more silicon lenses in between them in order to introduce a focus for imaging. Due to the fiber delivery, the two cases can be switched from transmission mode to reflection mode in minutes.

### **Miniature, packaged terahertz transmitter and receiver modules**

The heart of the entire system shown in Figures 1 and 2 is the packaged transmitter and receiver modules shown on the left hand side of Figure 3. These modules, which contain a low-temperature grown GaAs (LT-GaAs) antenna as the photoconductive element, also have a relay lens and fiber anchor inside of them. The fiber is permanently aligned to the THz antenna with sub-micron precision and the module is back-filled with an inert gas and then hermetically sealed using standard telecom packaging methods. The photoconductive device, which has a 2-mm bowtie antenna, is attached to a high-resistivity silicon, aplanatic hyperhemispherical lens which

helps couple the radiation out of the package efficiently without causing beam diffraction. The module is less than 1 inch long by ½ inch square and weighs only a few ounces. This THz module is robust and suitable for use in industrial remote sensing as well as in laboratory spectroscopy.

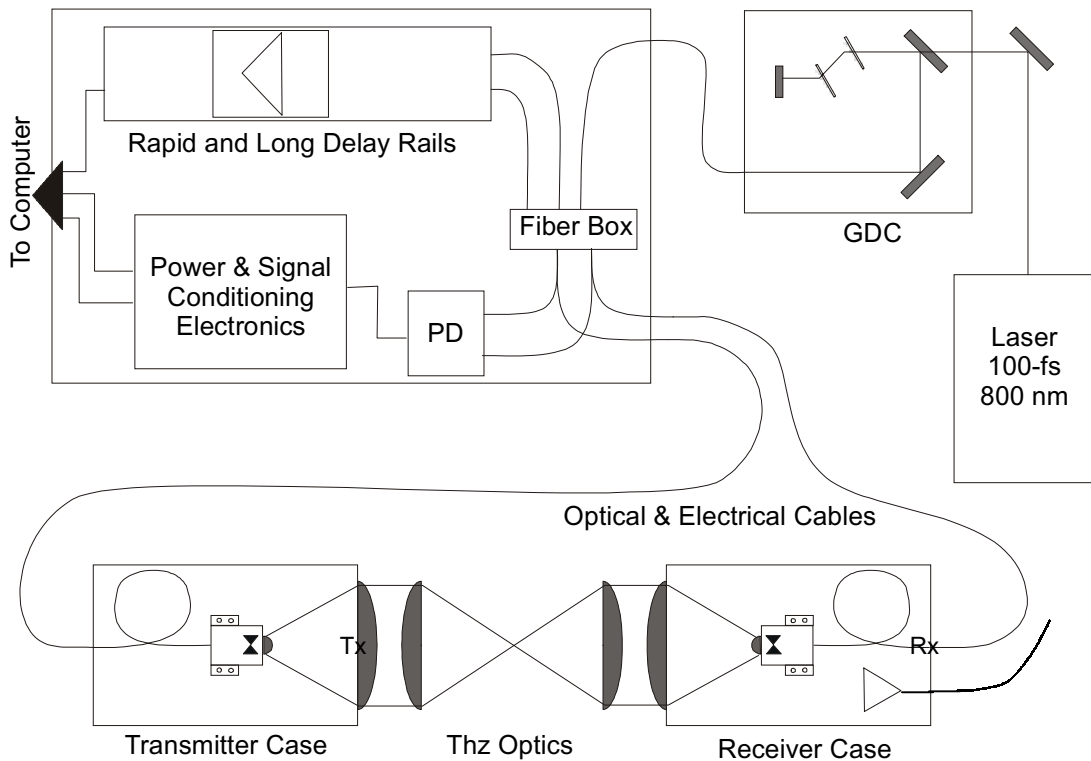


**Figure 2.** A schematic showing the components found in each of the boxes shown in Figure 1. The signals going to computer consist of the amplified terahertz signal, the position signal from both delay rails, and the photodiode signals. PD: two photodiodes. Dashed lines represent the terahertz beam.

The right hand image in Figure 3 shows a fiber coupled THz transmitter aligned with a conventional hi-resolution XYZ stage with differential micrometers. This laboratory unit is approximately 8 x 8 x 8 inches in dimension and weighs more than 5 pounds. It is still superior to previous THz transmitters in that the fiber coupling of the laser source does not rigidly constrain its location. This flexibility has been used to measure the beam patterns from both collimating and aplanatic substrate lenses in both the H and the E-planes from 0 to 50 degrees. Such a measurement would have been impossible using older, free-space systems.<sup>9</sup> However, such a laboratory demonstration unit remains impractical for commercial use since the femtosecond optical pulses must be manually focused with sub-micron precision onto the photoconductive LT-GaAs bow-tie THz antenna using bulky translation stages. Also, despite the precision of these mounts, they are still more susceptible to both vibration and thermal misalignments than the packaged modules.

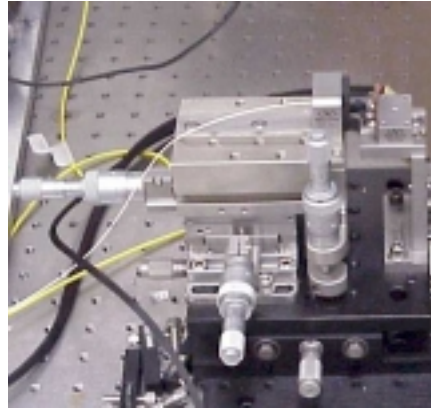
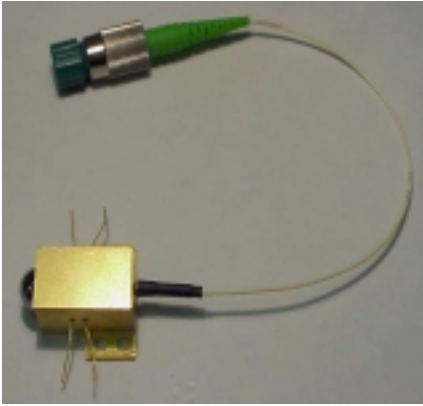


**Figure 3.** **Left:** A fiber-pigtailed T-Ray transmitter module measuring 1" x 0.5" x 0.5" and weighing only a couple of ounces. The silicon hyperhemispherical is visible on the left side of the module. **Right:** A fiber-coupled THz transmitter aligned with a conventional hi-resolution XYZ stage with differential micrometers. This laboratory unit is approximately an 8" cube and weighs more than 5 pounds. It is still superior to previous THz transmitters in that the fiber coupling does not rigidly constrain its location, as does conventional free space optics.

### System performance

The T-Ray system was used with 1 mW of optical power going to both the transmitter and the receiver. The bias on the transmitter was set at 24 volts and the receiver amplifier had a voltage gain of 500. The rapid shaker for this particular system gave a 30-ps excursion at a scan rate of 22 Hz. Figure 4 shows the temporal terahertz waveform, the noise on this waveform, and the signals Fourier transform. The dotted trace in all three graphs corresponds to a one-second-acquisition time, corresponding to 22 averages. The solid trace shows a 5-minute average, corresponding to 6,600 averages. Using the peak-to-peak voltage noise on the inset temporal graph, we obtain a signal to noise of about 600 to 1 for the one-second average and about 10,000 to 1 for the five-minute average. The 10% bandwidth for both traces extends from 0.03 to 1.5 THz with usable bandwidth to 2 THz in the one-second trace and past 3 THz for the 5-minute average. As evidence for this the water absorption lines at 2.64 and 2.77 THz are clearly visible. Looking at our data we find that the position of these lines to be accurate to within the 33 GHz resolution given by our 30-ps window.

While the signal to noise of this system is typical of other photoconductive and electro-optic terahertz systems, the optical power requirements, as well as the voltage requirements, are not. The system used to produce the results given above has used the same photoconductive elements as the transmitter and receiver for over a year without damaging a single one. Typical voltage damage to these devices occurred consistently at a bias of greater than 40 volts and more than 11 mW of optical power. By using them at such a reduced level, the longevity of these sensitive elements is assured.

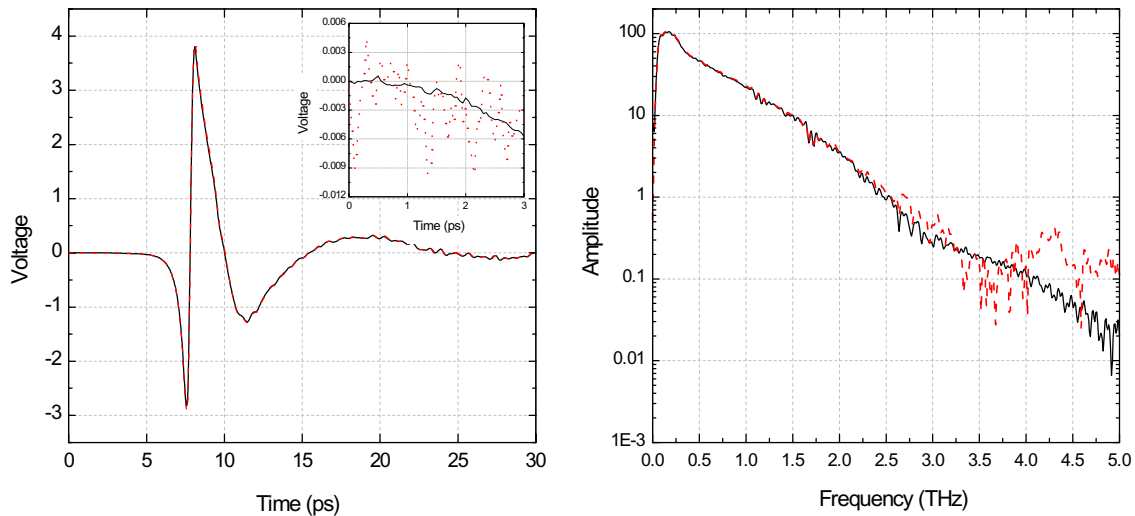


**Figure 4.** Shown are a one-second average (dotted line) and a five-minute average (solid line). The insert in the time graph shows the first 3 ps of the time data to show the noise in the two traces. The Fourier transform on the right shows accurate water absorption lines out to 2.77 THz.

### 3. IMAGING

Imaging is one of the most exciting applications of THz time-domain spectroscopy. T-ray images may be taken using transmission or reflection geometry. By analyzing the THz waveform in either the time domain (material homogeneity or thickness variations) or the frequency domain (frequency-dependent absorption) as well as by other methods, images identifying material properties can be constructed. Due to the huge spectral range of the time-domain system, looking at various places across the terahertz spectrum can form true hyperspectral images. Non-polar solids (such as plastics) are generally at least partially transparent in the 0.2 to 5 THz range. Non-polar liquids are transparent as well, whereas polar liquids, such as water, are highly absorptive. This is because absorption in the THz range of the electromagnetic spectrum is generally due to the rotational motions of dipoles within a material. Crystals formed from polar liquids are substantially more transparent because the dipolar rotations have been frozen out, however these crystals may exhibit phonon resonances in the THz range. Metals completely block THz pulses. Polar species within a gas may have sharp, strong rotational transitions in the THz range.

These T-Ray images can complement or replace existing imaging methods based on mid-IR or ionizing radiation. Furthermore analytical T-Ray images can be made of objects, which would be impossible using these conventional methods. For example polar species could be identified within the image of a flame, even in the presence of strong incoherent background radiation. This is because the photoconductive time gating of the

THz pulse provides extraordinarily good signal to noise by only sampling the ultrafast THz pulse. No thermal shielding or cryogenic cooling is required for a photoconductive THz detector.

Some examples of published T-Ray imaging applications include: identifying raisins in a box of cereal by water content; establishing the rate of water evaporation and uptake in leaves; examining circuit interconnects in packaged IC's; reading text in envelopes or beneath paint; identifying the number of almonds in a candy bar; identifying tooth decay; and locating watermarks in various currencies.<sup>10,11</sup> Not all of these images are what one might expect in a real-world application, and that is because, until now, T-Ray imaging has been restricted to researchers with the ability to hand-construct a complete THz imaging spectrometer. Understandably, most of the researchers taking these images were primarily concerned with the physics of THz generation and propagation. The images were taken more to illustrate THz science rather than to examine the properties of the imaged object. However, with the availability of a commercial turnkey T-Ray imaging spectrometer, T-Ray imaging and spectroscopy is accessible to those who want to examine the benefits of T-Ray imaging but who are not necessarily experts in the field.

The imaging described in the proceeding section was performed with reasonably simple computer control and much post-processing. In order to make this kind of terahertz imaging truly accessible to all users, an intelligent interface has to control the large amounts of data being generated by it. To address this need, we have developed a software system based on LabView that has the look and feel of a standard Windows<sup>®</sup> program and allows a user to not only take real time terahertz waveforms, but also allows one to do 2D imaging quickly and easily.

The software has four modes of operation: Rapid Scan, Long Scan, View Scans, and Image. The screen shot in Figure 5 shows the Rapid-Scan screen. On the left hand side of the screen is a control bar that allows the user to jump between these four modes of operation as well as enter the "Settings" screen, which allows the user to monitor the optical power in the transmitter and receiver fibers, enable or disable the imaging capabilities of the software, and setup the DAQ settings for the data acquisition card used.

In the Rapid Scan screen the user gets updates at a rate of about 5 Hz that allows one to do live tweaks to the system and also allows a user to setup for an image very rapidly. When averaging many traces the acquisition rate equals the scan rate of the shaker (about 20 Hz). The long slider bar across the top of the main graph corresponds to the shakers position on the long rail. This absolute time scale can be displayed on the rapid-scan time axis, which then allows the user to take a background trace at one spot on the rail, and then analyze data taken at a different spot further down the rail. For example, if the long rail was at 60 ps for the background trace, and then a thick sample was placed in the beam, the user could simply move the long rail (by dragging the position box or by typing in a long rail position), and then determine the total delay by tracking the

background with one cursor and the transmitted pulse with the other. This frees the user from having to do long scans, which are plagued by low-frequency noise and long-term drift, but still allows them to take advantage of the full one-nanosecond of delay offered by the long rail. There are times, however, when a long scan is absolutely necessary, for instance, when trying to get fine resolution of sharp resonances, or when looking at complicated pulses that last for more than 40 ps.

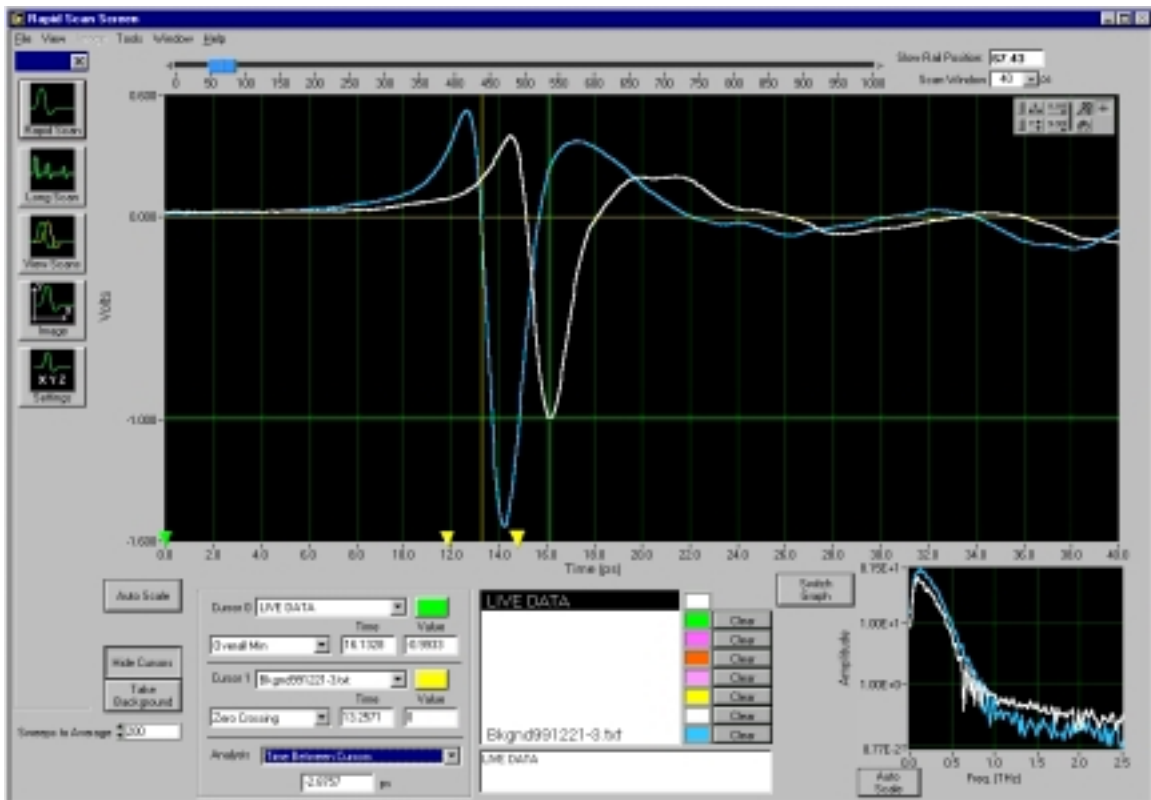


**Figure 5.** Rapid-scan acquisition screen for the time-domain terahertz spectrometer software. The main graph shows two time-domain traces. The white trace is the live, rapidly updated THz scan which has passed through a latex balloon. The gray trace is a saved background scan. The secondary graph shows the Fourier transforms of the two traces.

The THz image acquisition and display screen for our imaging spectrometer is shown in Figure 6. As in Figure 5, the control bar to the left allows the user the ability to jump between the various modes of operation. In the image screen the user has the choice of either setting up for and collecting an image or loading a previously taken image and re-analyzing it using new criteria. In order to acquire an image, the user usually first looks at the sample in various locations and sets up the cursors to examine the parameter of interest such as was done in Figure 5. Once this is done, the user then sets up the



parameters of the image consisting of the starting point, size, resolution, and number of averages for the desired image.

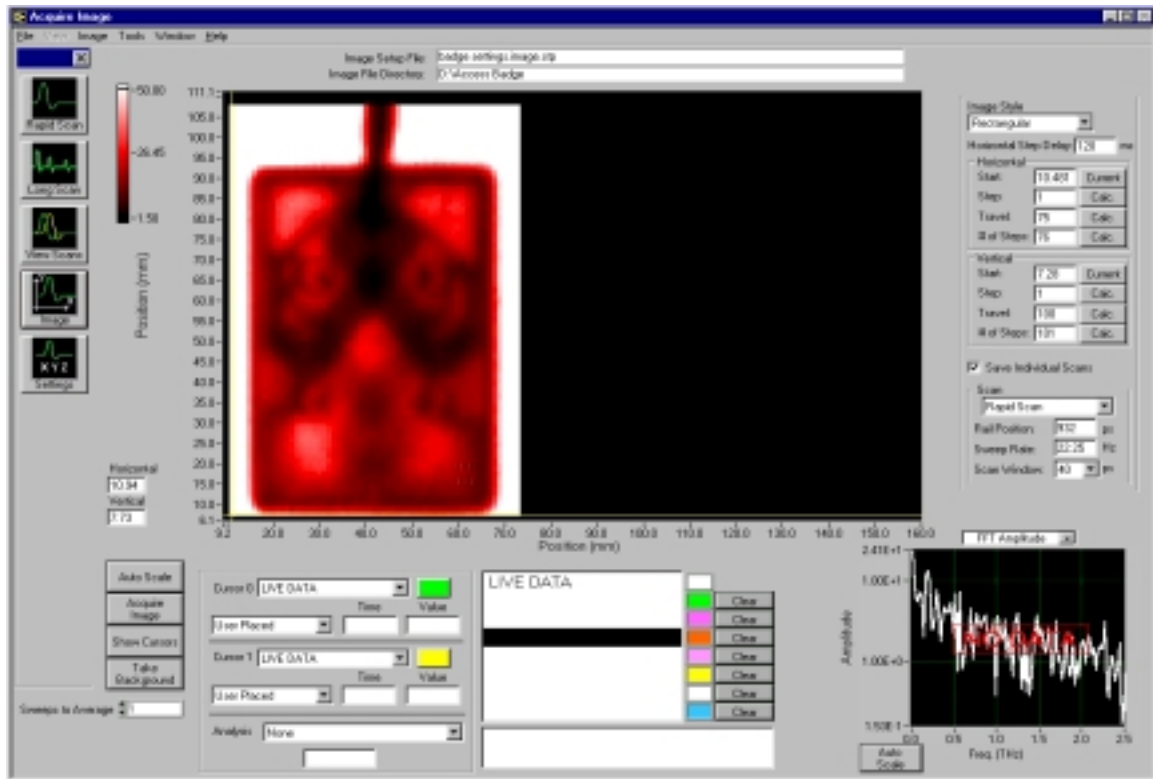


**Figure 6.** Software’s image-acquisition and display screen. The user sets the image size and resolution in the upper right. The full T-Ray waveform is stored for each pixel. The waveform for the pixel under the image cursor is shown in the lower left. In this case the cursor is on a pixel without any data corresponding to it, so the screen is only showing the live data. The image shown is a transmission image of the integrated electric field from 0.4 to 2.0 THz.

The T-Ray image shown in Figure 6 is a transmission image of a commonly used passive RF proximity access card (the vertical rectangle at the top of the card is the support clip). The card is an opaque ABS polycarbonate laminate with a Lexan skin measuring  $85.5 \times 53.9 \times 2.5\text{mm}^3$ . Interior to the card is a metallic inductor and antenna structure, which is unique to each card.

To generate a T-Ray image using the software, the user sets the rectangular scan matrix size and resolution (upper right hand corner Figure 6). The image in Figure 6 was scanned at a resolution of 75 X 100 pixels in 1-mm steps for a total of 7500 pixels. The user chooses an initial analysis; here the integrated electric field from 0.4 to 2.0 THz was chosen. Other frequency or time domain analyses could have been chosen. The software is also capable of generating a 1 dimensional time sequence image or graph. The user presses the “Acquire” button and the object is scanned automatically and the image is

generated. The full THz waveform is stored for each pixel. This allows multiple image analyses to be performed on the same image data set without having to re-scan the object.

#### 4. CONCLUSION

We have developed a time-domain terahertz system based on fiber-pigtailed, hermetically sealed modules that will allow users unskilled in ultrafast photonics to do terahertz spectroscopy and terahertz imaging. This system needs less than 10 mW of optical power and has nearly two decades of spectrum extending from 0.03 to 2 THz. The integrated nature of this system, with its turnkey operation and user-friendly software should help push the use of THz technology and ultrafast optics to new and hitherto unexplored markets.

#### ACKNOWLEDGEMENTS

This work has been partially supported under the Air Force SBIR Initiative, Contract No. F33615-98-C-2820 and contract monitor J. R. Gord.

#### REFERENCES

1. M. C. Nuss and J. Orenstein, *Millimeter and Sub-millimeter Spectroscopy of Solids*, Ch. 2, Springer-Verlag, Berlin, 1998.
2. D. Grischkowsky, S. Keiding, M. van Exter, and Ch. Fattinger, "Far-infrared time-domain spectroscopy with terahertz beams of dielectrics and semiconductors," *J. Opt. Soc. Am. B* **7**, p. 2006, 1990.
3. J. T. Kindt and C. A. Schmuttenmaer, "Far-infrared dielectric properties of polar liquids probed by femtosecond terahertz pulse spectroscopy," *J. Phys. Chem.* **100**, p. 10373, 1996.
4. J. E. Pedersen and S. R. Keiding, "THz time-domain spectroscopy of nonpolar liquids," *IEEE J. Quantum Elect.* **28**, p. 2518, 1992.
5. R. A. Cheville and D. Grischkowsky, "Far-infrared terahertz time-domain spectroscopy of flames," *Opt. Lett.* **20**, p. 1646, 1995.
6. D. M. Mittleman, R. H. Jacobsen, and M. C. Nuss, "T-Ray Imaging," *IEEE J. Quantum Electron.* **20**, p. 679, 1996.
7. P. Coy, "Beyond X-Rays: T-Rays measure content," *Business Week*, p. 11, July 10, 1995. R. Lipkin, "T-Rays for Two," *Science News* **148**, p. 136, 1995.
8. B. Atherton, private communications.
9. D. Mittleman and J. V. Rudd, to be published.
10. Q. Chen, Z. Jiang, and X.-C. Zhang, "All-optical THz imaging," *SPIE Conference on Terahertz Spectroscopy and Applications*, SPIE vol. **3617**, p. 98, 1999.
11. D. M. Mittleman, M. Gupta, R. Neelamani, R. G. Baraniuk, J. V. Rudd, and M. Koch, "Recent advances in terahertz imaging," *Appl. Phys. B* **68**, p. 1085, 1999.